Assessing the accuracy of OB star mass-loss rate measurements using high-resolution X-ray spectroscopy

Maurice Leutenegger
(NASA/GSFC/CRESST/UMBC)
with D. Cohen, S. Owocki, many others

Outline

- Motivation – mass loss rate measurements
- Method – shape of X-ray emission line profiles
- Results – comparison with other wavelengths; reliability of mass loss rate measurements

Mass loss rates are very important

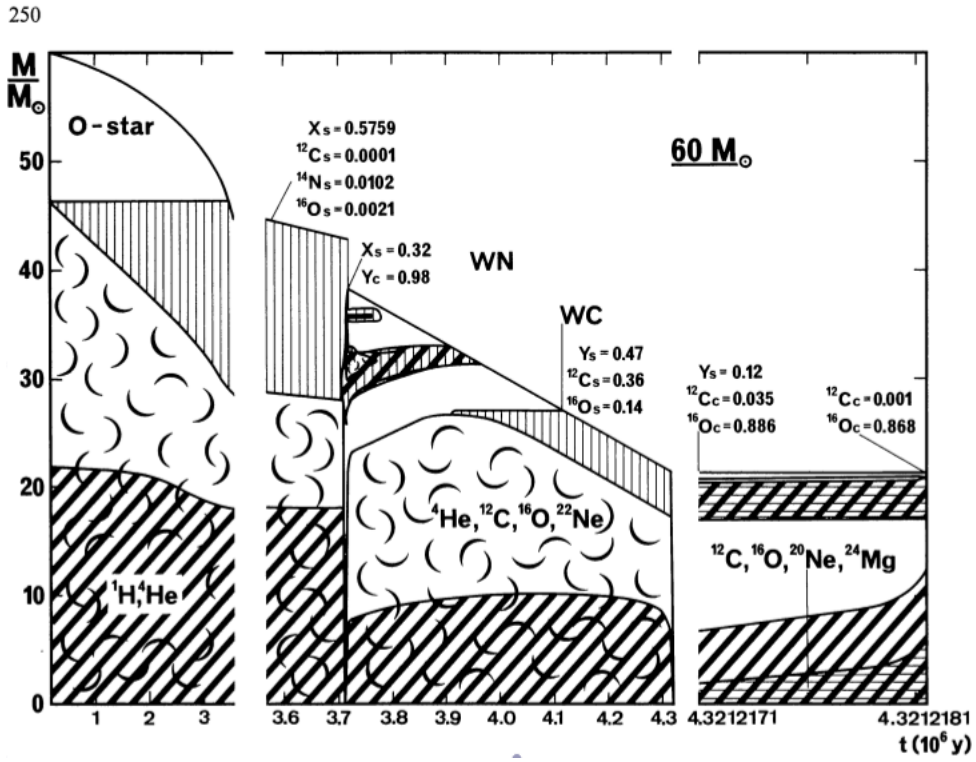

Meynet & Maeder:
stellar evolution is influenced by mass loss

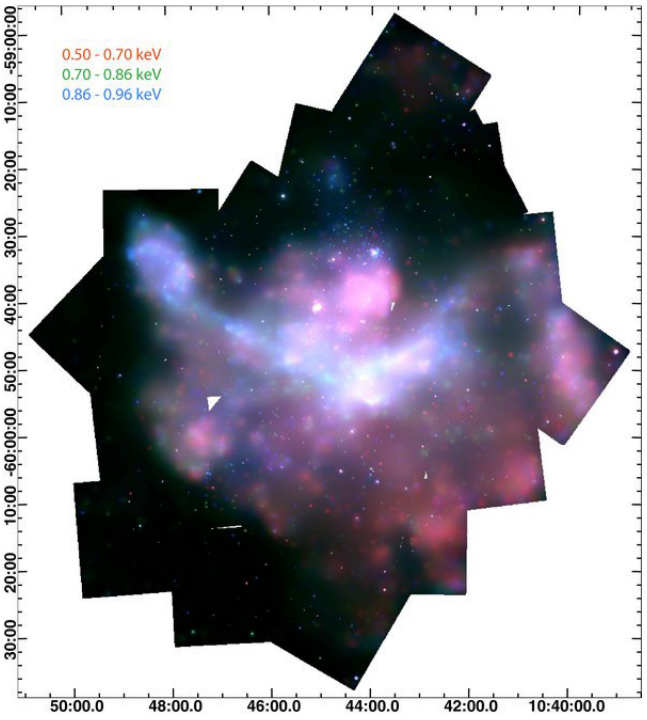

Townsley et al.: Carina nebula diffuse X-ray emission from hot gas heated by mechanical energy input from stellar winds (energy budget)

Optical/UV/IR/Radio diagnostics all have large systematic uncertainties

- Hα and radio free-free emission scale with density squared -> clumping
- UV resonance absorption lines depend on ion balance
- Even unsaturated UV resonance absorption lines from dominant ions may be affected by nonmonotonic velocity fields
- Systematics can be >~ factor of 3-10

Large discrepancy between UV resonance lines and radio/Hα

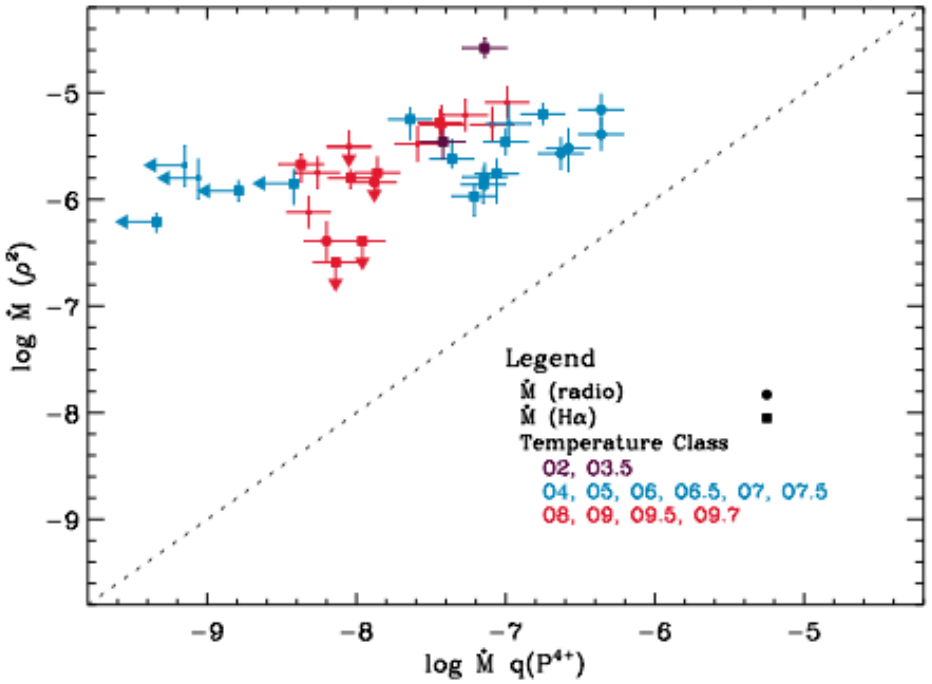

FIG. 3.—Comparison of $\dot{M}$ with $\dot{M}q(P^{+4})$. The shapes of symbols distinguish radio (*circles*) and Hα (*squares*) measurements, while symbol size separates the primary (*large*) and secondary (*small*) samples. Upper limits on nondetections are indicated by arrows. Color coding divides the entire sample into early (O2, O3, O3.5), mid (O4–O7.5), and late O types (O8–O9.7). The dotted line denotes a 1:1 correlation between the two measurements.

Fullerton et al. 2006:
P V lines are not saturated,
indicate much lower mass loss rate

Outline

- Motivation – mass loss rate measurements
- Method – shape of X-ray emission line profiles
- Results – comparison with other wavelengths; reliability of mass loss rate measurements

X-rays from radiatively driven winds

- Wind is driven by radiation pressure in UV lines, which is unstable
- This leads to shocks and X-ray generation
- Most of wind is "cool" (of order photospheric temp.), but small fraction is heated to ~1-10 MK

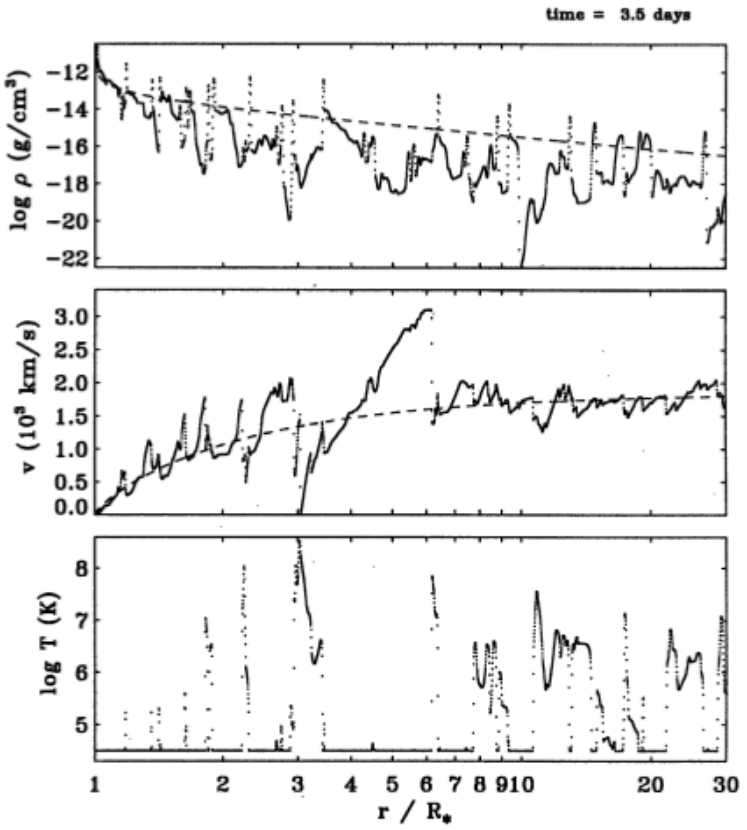

Fig. 7. Snapshot of the wind structure 3.5 d after model start. The photospheric disturbance is a tunable sound wave.

Feldmeier et al.

X-ray profile asymmetry measures wind optical depth

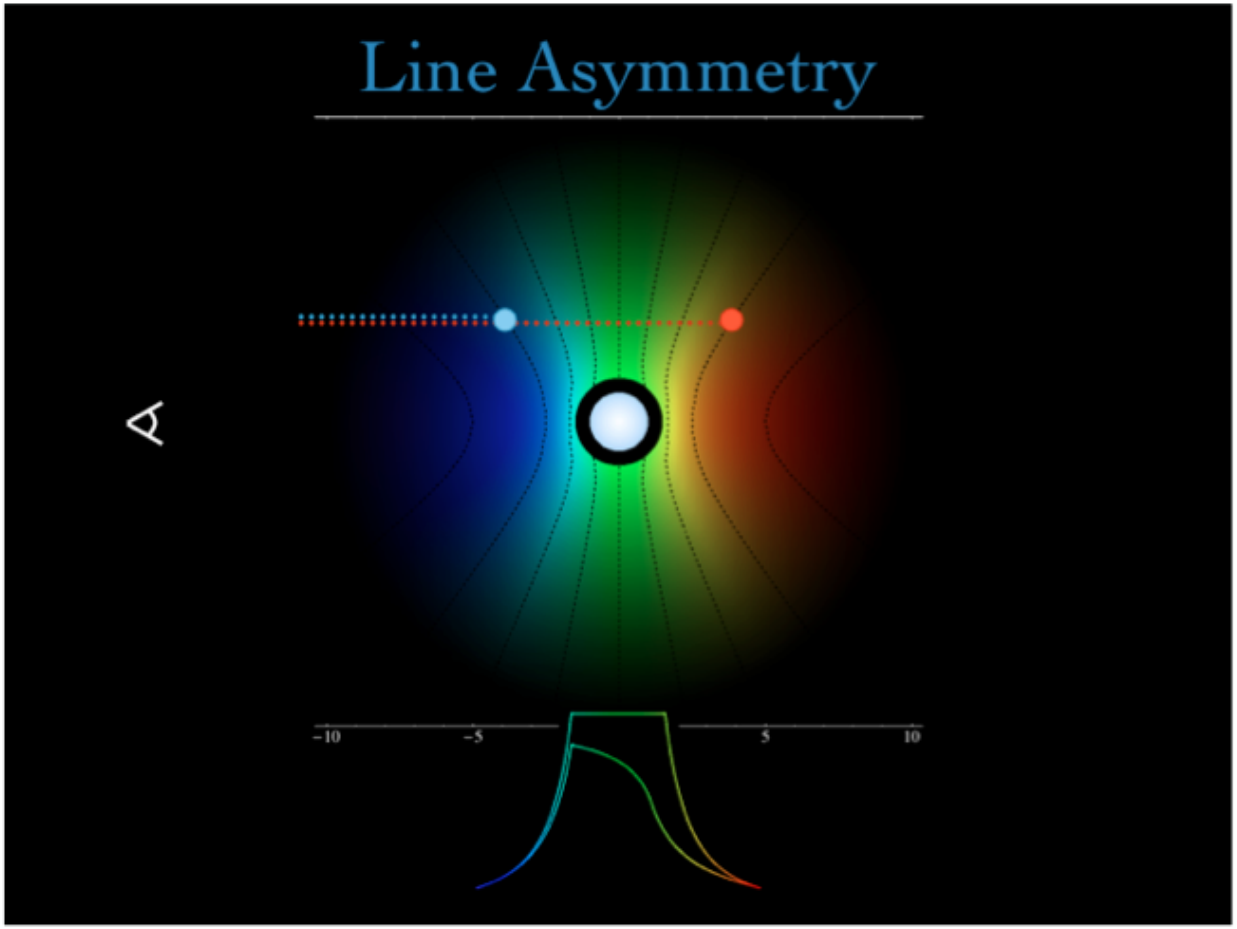

Profile formation

$$L_\lambda = 4\pi \int dV \eta_\lambda e^{-\tau}$$

$$\tau(p,z) = \int_z^\infty dz' \kappa(\lambda)\rho(r')$$

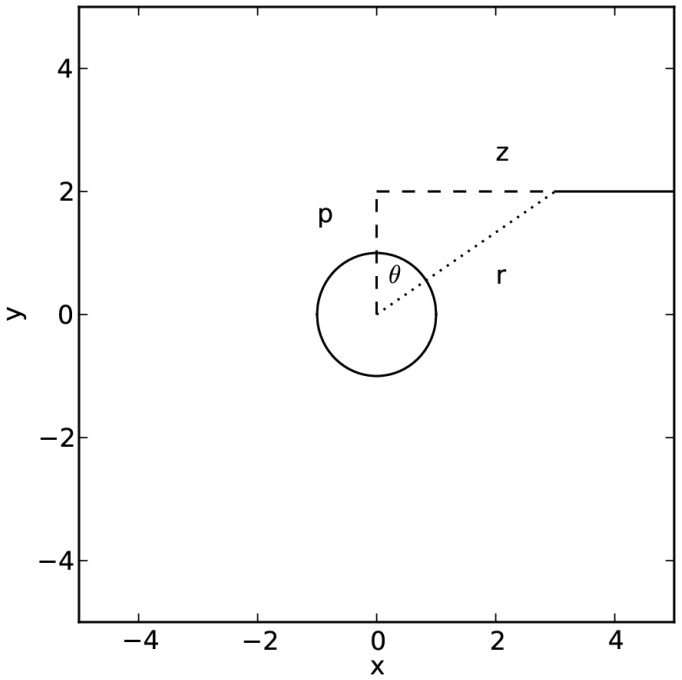

Diagram of ray coordinates (p,z)

Profile formation

$$\tau(p,z) = \int_z^\infty dz' \kappa(\lambda)\rho(r')$$

$$\rho(r) = \frac{\dot{M}}{4\pi r^2 v(r)}$$

$$\tau(p,z) = \tau_* t(p,z)$$

$$\tau_* = \frac{\kappa \dot{M}}{4\pi R_* v_\infty}$$

X-ray profile asymmetry measures wind optical depth τ_*

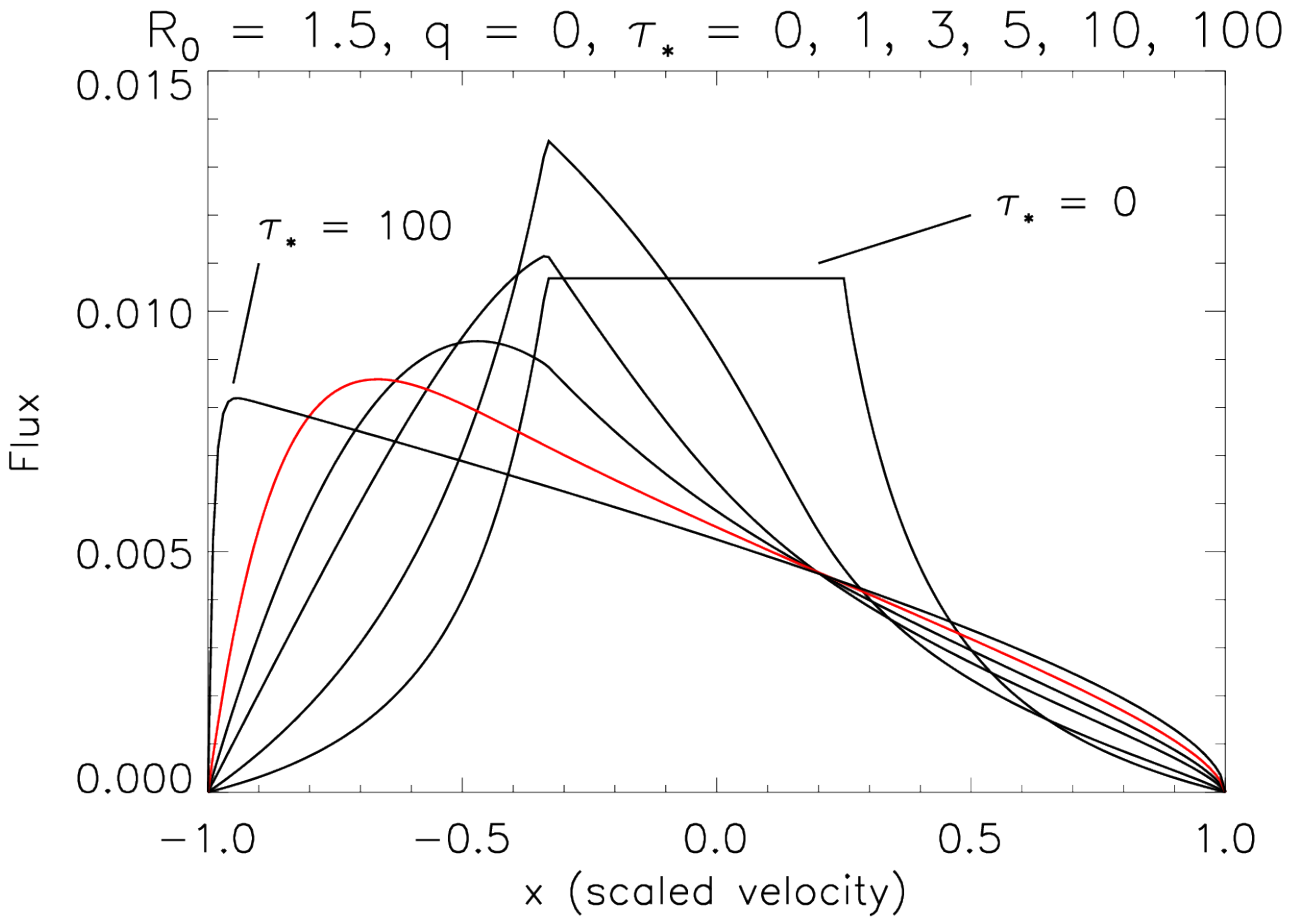

X-ray profile asymmetry measures wind optical depth τ_*

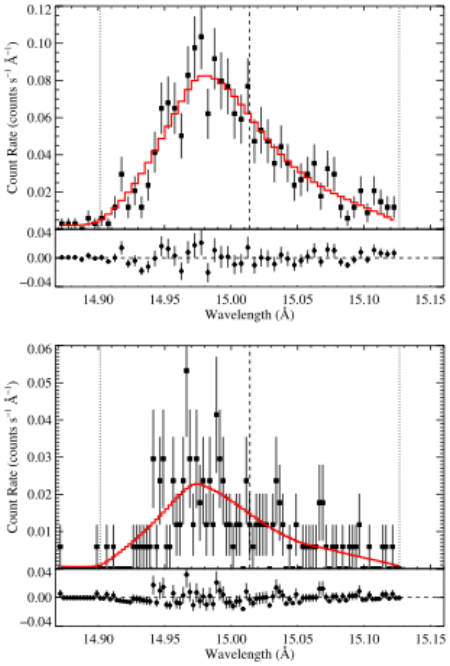

Figure 3. The Fe XVII line at 15.014 Å in the MEG (top) and HEG (bottom), with the best-fitting model superimposed. We have not done any rebinning of the data. The error bars represent Poisson, root-N, statistics. The dashed vertical lines indicate the laboratory rest wavelength of the emission line, and the two dotted vertical lines in each panel indicate the wavelengths associated with the Doppler shift due to the stellar wind terminal velocity of 2250 km s^{-1}. The model is shown as the thick (red) histogram, while the data are shown as (black) solid squares with error bars. The fit residuals are shown in the horizontal windows below the data, with the same one sigma error bars that are shown with the data.

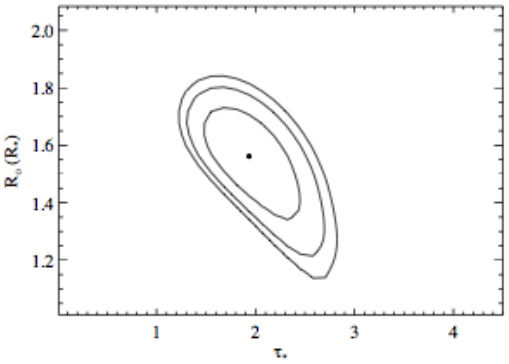

Figure 4. Confidence contours (68, 90, and 95 percent) for the model fitting of the the Fe XVII line at 15.014 Å. The best fit, shown in Fig. 3, is represented by the filled circle.

Cohen et al. 2010

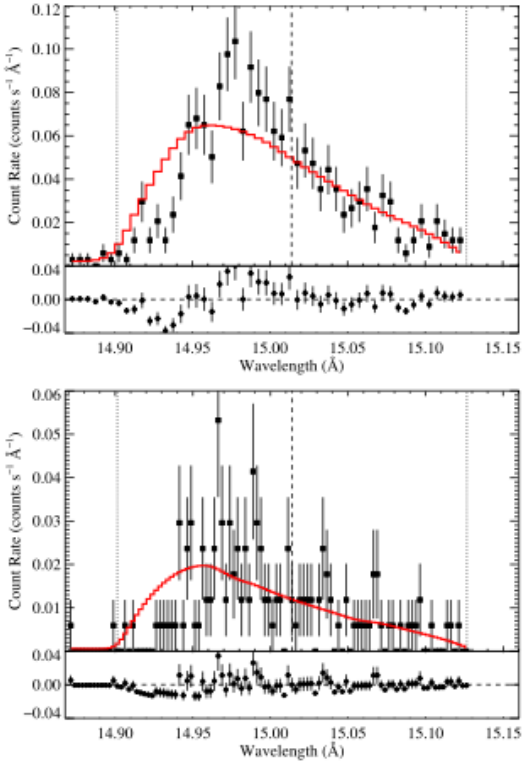

Figure 5. The Fe XVII line at 15.014 Å in the MEG (top) and HEG (bottom), with the best-fitting model having $\tau_* = 5.30$ superimposed. This is the value implied by the smooth-wind Hα mass-loss rate and our wind opacity model. The normalization and R_o were the adjustable parameters of this fit. Even this best-fitting model is statistically unacceptable.

Can do this for all lines

- Best fit for all lines in Chandra HETGS spectrum of ζ Pup
- τ^* is proportional to κ, $\dot{M}$
- Mass loss rate is reduced by factor of ~2.5

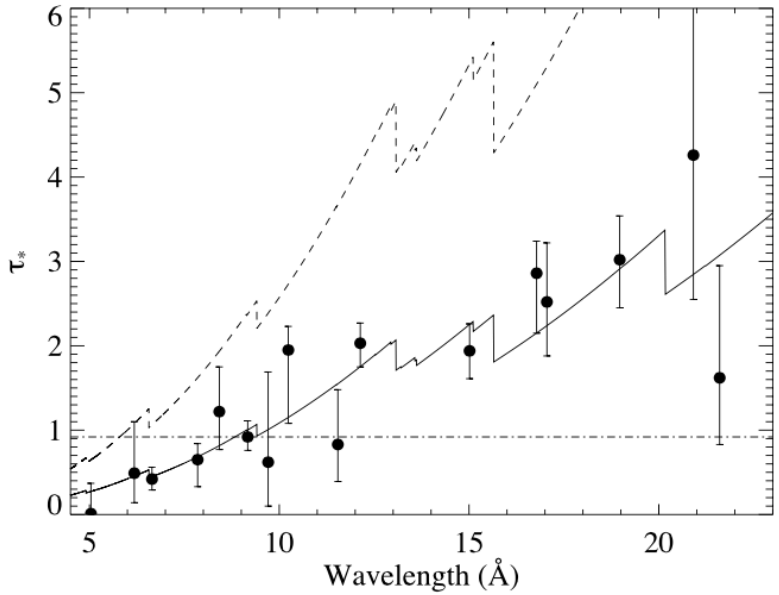

Cohen et al. 2010

Can apply same method to other stars

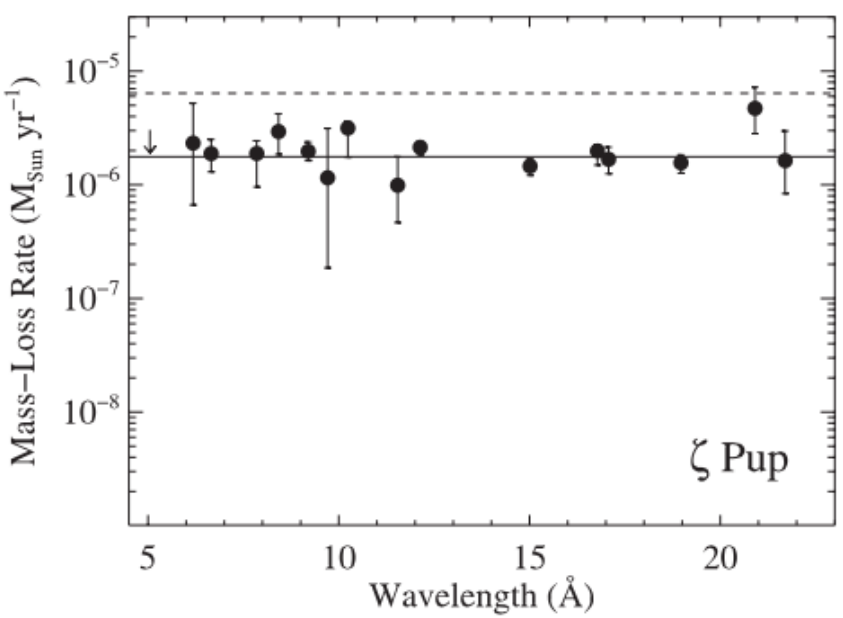

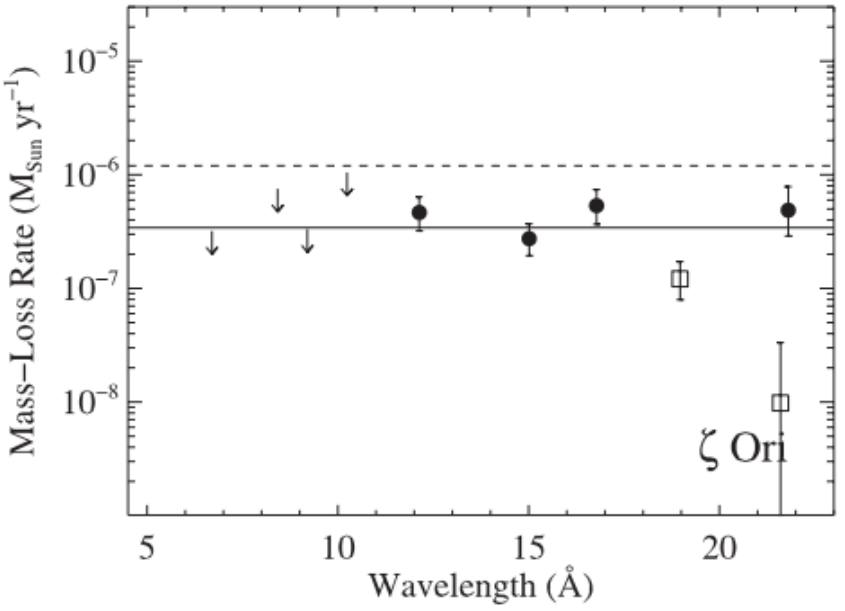

Cohen et al. 2014

(Opacity has been divided out in these plots)

Can apply same method to other stars

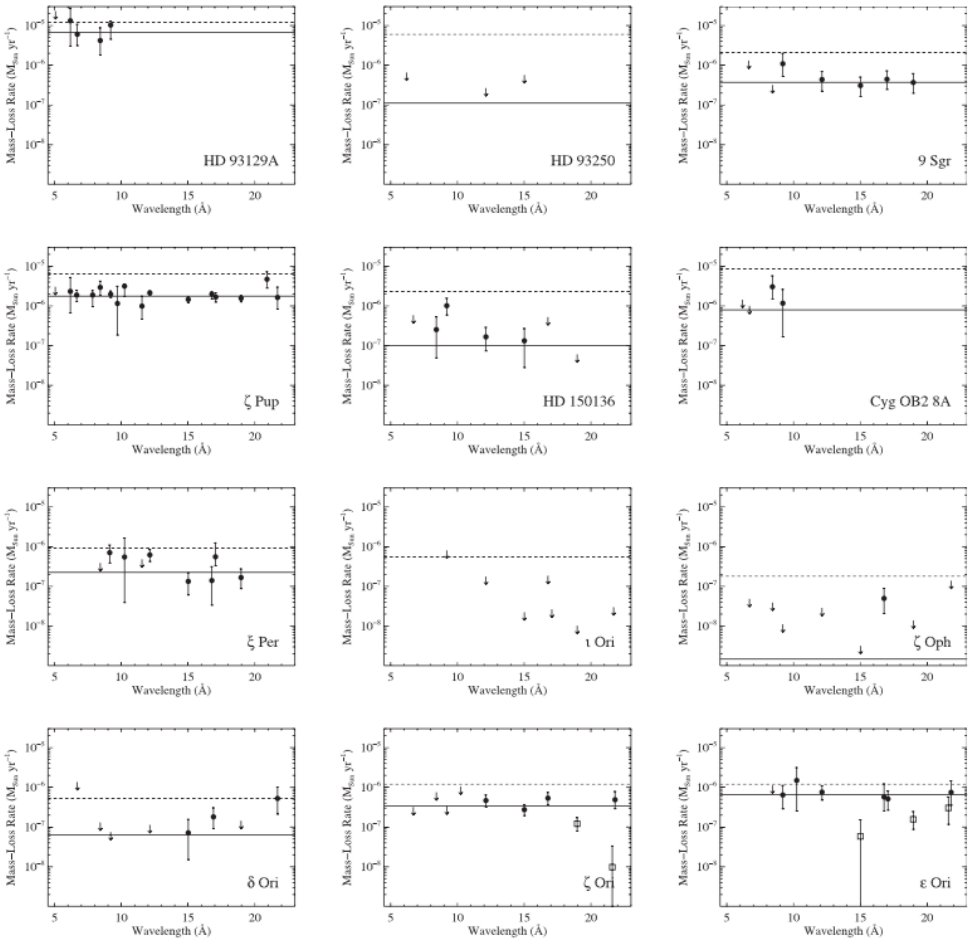

Cohen et al. 2014

Outline

- Motivation – mass loss rate measurements
- Method – shape of X-ray emission line profiles
- Results – comparison with other wavelengths; reliability of mass loss rate measurements

Comparison with theory (as a proxy for other wavelengths)

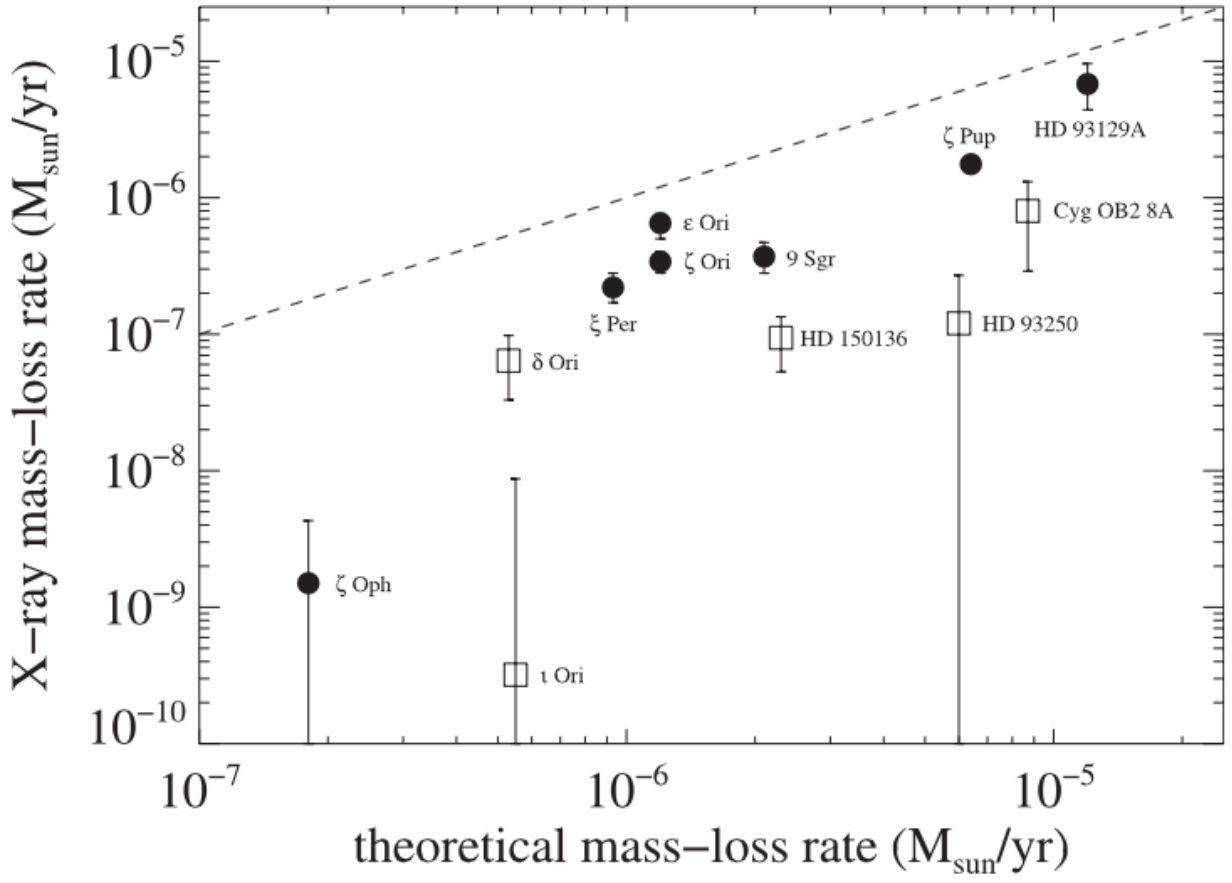

Theory values from Vink et al. (2000)

Outline

- Motivation – mass loss rate measurements
- Method – shape of X-ray emission line profiles
- Results – comparison with other wavelengths; reliability of mass loss rate measurements

Factors affecting X-ray measurements

- Statistical uncertainty
- Systematic wavelength uncertainty
- “Missing” physics / approximations (e.g. satellite or other weak lines, radial dependence of opacity)
- Assumptions / “interesting” physics: porosity/ wind structure, radial plasma distribution, resonance scattering, ...

Factors affecting X-ray measurements

- Statistical uncertainty
- Systematic wavelength uncertainty
- “Missing” physics / approximations (e.g. satellite or other weak lines, radial dependence of opacity)
- Assumptions / “interesting” physics: porosity/ wind structure, radial plasma distribution, resonance scattering, ...

Effect of systematic wavelength shift

- Use ζ Pup Fe XVII 15.014 Å as example
- Chandra MEG systematic uncertainty is 1.5 mÅ at 15 Å
- Change in τ_* is 0.13 / mÅ, so systematic uncertainty in τ_* is 0.2, which is about 10%

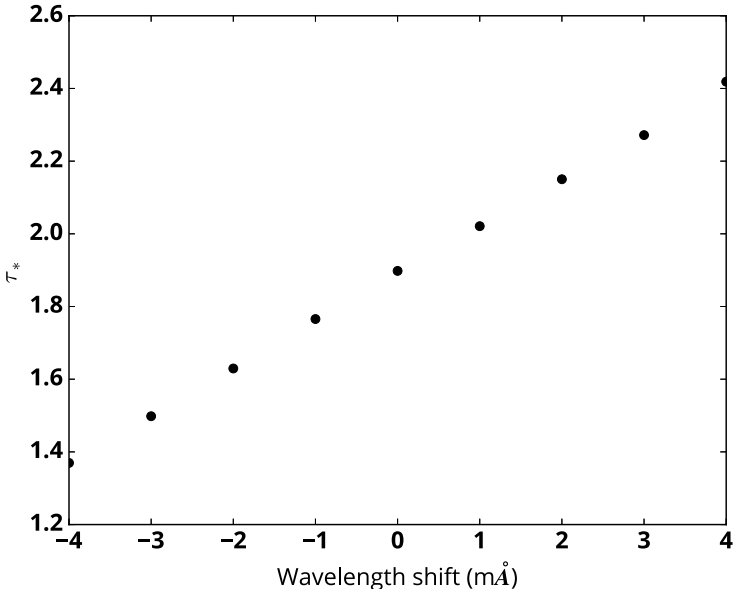

Porosity – reduction in effective optical depth due to large clumps

"Pancake" shaped clumps: anisotropic porosity

Feldmeier et al. 2003
Oskinova et al. 2005,2006,

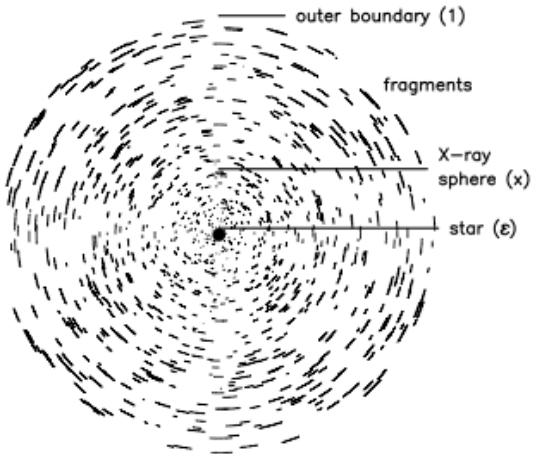

Fig. 1. Fragmented wind, with $N = 10$ fragments per radial ray. The symbols in brackets designate radii.

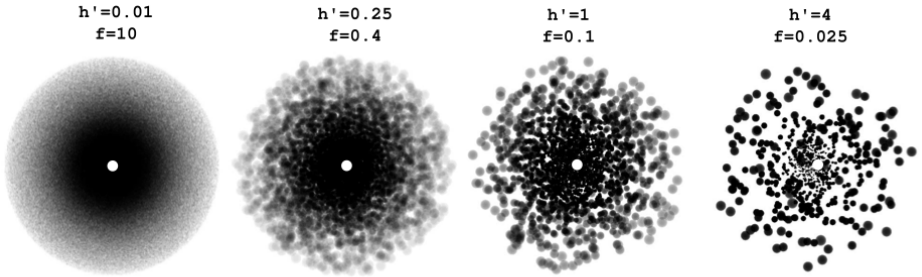

FIG. 3.—Explicit manifestation of clump structure in models set to have statistical properties corresponding to porosity length scale factors $h' = 1/100$, 1/4, 1, and 4. The individual clumps have a diameter that increases with radius as $\ell = 0.1r$, leading to radially-fixed volume filling factors $f = \ell'/h' = 10$, 0.4, 1, and 0.025, respectively. The leftmost panel, with the smallest porosity length, corresponds nearly to a completely smooth wind case. In each panel, the gray-scale level is proportional to the transmission of a uniform illumination from the back, i.e., as $\exp[-\tau]$, where τ is the integrated optical depth along any given line of sight. The optical thickness of individual clumps decreases outward, with an overall level corresponding to a total wind optical depth parameter $\tau_* = 5$. These visualizations assume that the viewer is at infinity, so the apparent size of each clump is proportional to its linear scale, without any perspective effect; clumps that appear smaller actually are smaller, because they are at smaller radii. For context, the central white disk illustrates the size and location of the central star, and for clarity, only clumps within the central 20 R_* are included.

"Ball" shaped clumps: isotropic porosity

Owocki & Cohen et al. 2006
(Fig. by R. Townsend)

Effects of porosity

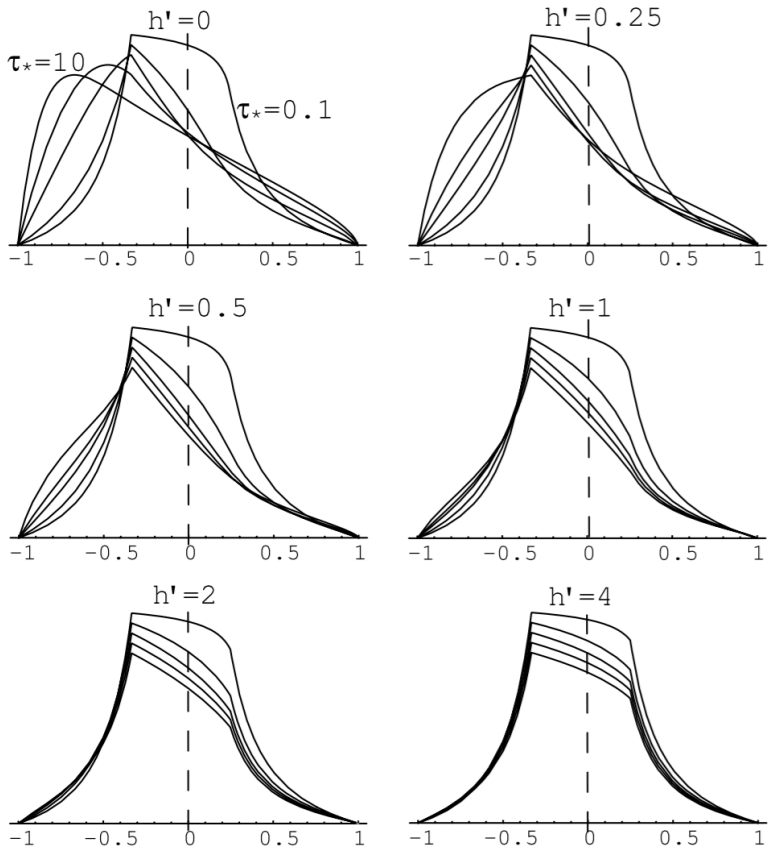

- Key parameter: porosity length (h) – mean free path between clumps
- Higher porosity leads to more symmetric profiles for the same mass-loss rate...
- or higher mass-loss rate for the same profile (shape is degenerate to zeroeth order)

Porosity is constrained

- Porosity lengths greater than ~ R_* are disfavored theoretically
- Also disfavored by HMXB variability studies (e.g. Grinberg et al.) and lack of variability in X-ray emission of O stars (e.g. Nazé et al.)
- Also disfavored by subtle changes in O star line profile shape not seen in high S/N data (e.g. Leutenegger et al. 2013)

Effect of iso porosity with $h_\infty = R_*$

- Typical increase in Ṁ is of order 10-40%
- Effects are stronger for stars with higher Ṁ

(Please compare blue and red points)

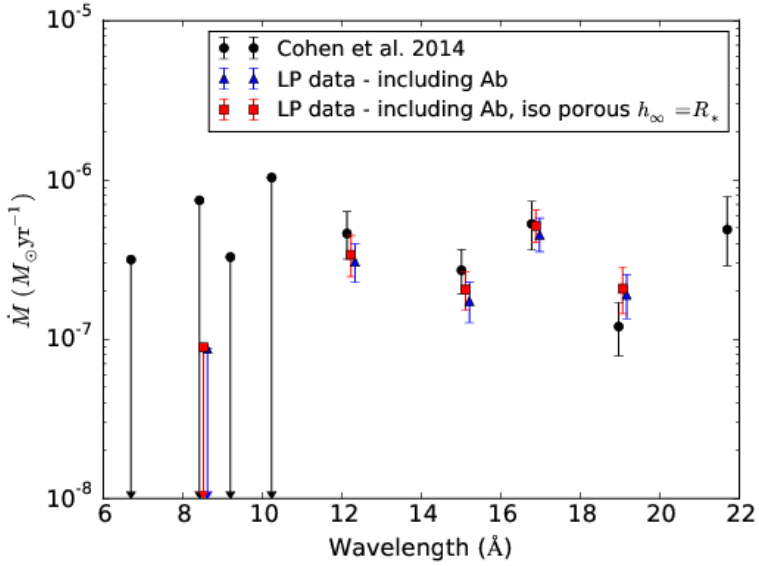

data are from Chandra LP on ζ Ori

Summary

- X-ray derived mass loss rates of OB supergiants are a factor of a few lower than theory (based on observations from other wavelength bands)
- Understanding and minimizing uncertainties, especially in modeling, is crucial
- The overall systematic error in the x-ray mass loss rates is estimated at the level of 50% or lower